
Effect of local slopes of roughness during contact between solids

Abdeljalil Jourani* — Alexandre Dellaleau* — Michel Dursapt*
Hedi Hamdi* — François Sidoroff** — Hassan Zahouani*

*,** *Laboratoire de Tribologie et Dynamique des Systèmes, UMR 5513, CNRS*

* *E.N.I.S.E, 58, rue Jean Parot
F-42023 Saint-Etienne cedex 02*

** *E.C.L, 36 avenue Guy de Collongue
F-69134 Ecully cedex*

ABSTRACT. In this work we propose to deal with the study of static sealing. The latter is modelled in a microscopic scale with finite elements method. The numerical simulations are related to the contact between conical asperities of a rough surface and a smooth rigid plan. It thus makes it possible to observe the local behaviours of the asperities during their crushing and to draw conclusions on the influence of various parameters such as the attack angle. If it is possible to deal with only a few asperities, the finite elements method does not allow us to succeed a full three-dimensional study. We thus propose in this work a simplified approach to solve this contact problem and to perform its generalisation to a random morphology. This useful method considers the contact between the real surface, which roughness is modelled as a distribution of indenters with various attack angles, and a smooth rigid plan.

RÉSUMÉ. Nous nous proposons dans cet article d'étudier le problème de l'étanchéité statique. Celui-ci est considéré à une échelle microscopique et modélisé à l'aide de la méthode des éléments finis. Les simulations numériques réalisées consistent à observer le contact entre les aspérités de la surface rugueuse et un plan rigide parfait. Ceci nous permet alors d'étudier le comportement local des aspérités lors de l'écrasement, ainsi que l'influence de divers paramètres comme leur angle d'attaque. S'il est possible de réaliser de telles études en modélisant quelques aspérités seulement, la méthode des éléments finis ne permet pas de simuler un contact tridimensionnel complet. Nous proposons donc dans cette étude une approche simplifiée afin de traiter ce problème de contact et de le généraliser à des géométries aléatoires. Cette nouvelle méthode propose la modélisation du contact entre la surface réelle, dont la rugosité est idéalisée à l'aide d'indenteurs aux angles d'attaque variant, et un plan rigide parfait.

KEYWORDS: rough surfaces, finite elements modelling, pressure distribution, asperities, crushing, static sealing.

MOTS-CLÉS: surfaces rugueuses, modélisation par éléments finis, distribution des pressions, aspérités, écrasement, étanchéité statique.

1. Introduction

To understand the phenomena which occur during the contact of two bodies is a key point to apprehend the static problem of sealing. This problem deals with multi scale property of roughness which must be taken into account in the whole behaviour of the system. Indeed, we can distinguish different observation levels. A macroscopic scale (form defect), mesoscopic (waviness defect), and microscopic (roughness). The modelling of the contact on a macroscopic scale is well established with Hertz and Boussinesq theory. On the contrary the contact study on a microscopic scale is much more difficult to apprehend.

In this paper we propose to study the local scale effect of roughness and slopes on contact problem. By comparison with the spherical model of roughness introduced by Greenwood and Williamson model (Greenwood *et al.*, 1966) to study statically the elastic contact. However, our work shows that a conical geometry of roughness fit better the experimental phenomena observed (Jourani *et al.*, 2003). The contact between two surfaces is thus modelled as the contact between a conical asperity Figure1 and an rigid plan (we thus use the geometrical and the behavioural equivalence principles (Johnson, 1984) suitable for tribology).

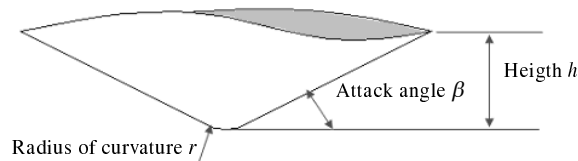


Figure 1. *Geometry of an asperity*

2. Crushing of an asperity

In order to observe the specific dimensions relating to the three parameters presented, we carried out measurements on three types of surfaces: milled, sand blasted and rectified ones. These measurements enabled us to define the framework of our study. That is the reason why the asperity modelled shows a height of $20\mu\text{m}$, an attack angle of 10° and a curvature radius of $10\mu\text{m}$. As the geometry of the asperity is defined, let us present the model realized by finite elements method with SYSTUS software (Systus user manual, 2004).

Due to the revolution symmetry of an asperity, we performed a two dimensional axisymmetrical model. The mechanical behaviour considered is elastoplastic with non linear isotropic hardening, see equation 1.

$$\sigma = \begin{cases} E \varepsilon \rightarrow \sigma < \sigma_y \\ R \varepsilon^n \rightarrow \sigma \geq \sigma_y \end{cases} \quad [1]$$

The Young's modulus is equal to 210GPa, the Poisson's ratio and hardening coefficient to 0.3. The elastic limit (σ_y) is 300MPa.

The substrate supporting the asperity shows mechanical behaviours similar to the latter, and proportions enabling us not to be subject to the influence of the boundary conditions. The calculations are performed in a large strains/large displacements option using an updated Lagrangian formulation. At each step non linear finite elements equations at equilibrium are solved using a Newton Raphson method. To deal with the contact we used a penalties method. The friction phenomena are not analysed in this study.

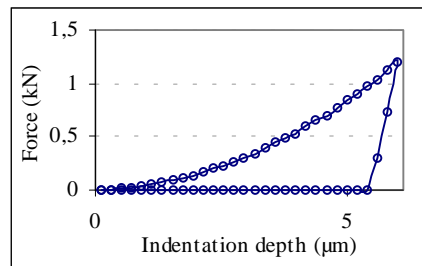


Figure 2. *Strength/depth curve for the crushing of the modelled asperity*

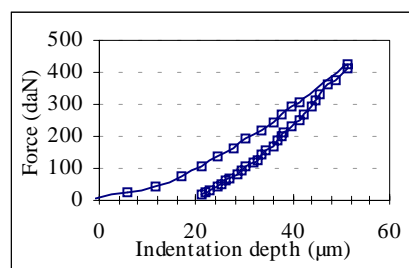


Figure 3. *Strength/depth curve for the crushing of a milled real surface*

The observation of the values and distributions relating to the stresses and the strains can be interesting to understand the phenomena of the crushing of an asperity, but the study of the strength/depth curve Figure 2 gives us many information (as the remanent depth, the normal stiffness, the strains energies, the real contact surface...).

The aim of this study is to understand the phenomena that appear during the crushing of a real surface. Now, let us observe the results relating to the crushing of an actual milled surface Figure 3. This evolution presents a rigorously different evolution from that observed with the finite elements model. Indeed the existing relation between plastic and elastic strains energies indicates that the experimental system reacts differently to the stresses applied. This significant difference can be interpreted in different ways. Among these two explanations are particularly distinguished. The first relates to the evolution of the plastic strain according to the attack angle of the asperity. In this, we evoke in particular the ideas presented by Tabor and Johnson (Johnson, 1984) concerning the concept of representative strains for the framework of the conical indentation. This concept will be then developed further in this study. Thus if the attack angle of the asperity increases the rate of plastic strain does too. The more acute the rake angle is, the more rapidly it evolves in an elastoplastic way.

3. Crushing of a multi asperity system

This model is based on the considerations and the assumptions exposed in the previous section. The geometry defined for this study authorizes us to interpret the results only in the case of the crushing of a milled surface Figure 4. The principle consists in crushing simultaneously three asperities whose geometries are identical.

This interpretation is based on the one hand on the observation of the von Mises equivalent stresses, and on the other hand on the interpretation of the results relating to the strength/depth curve.

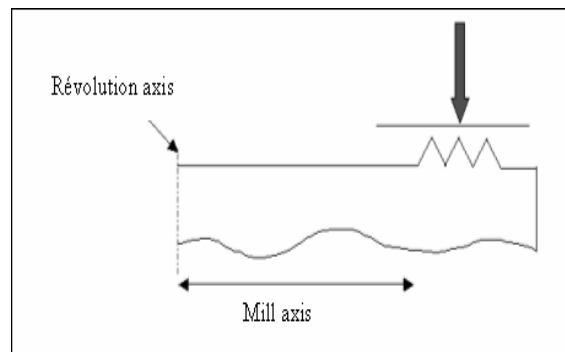


Figure 4. *Modelling of multi asperities crushing*

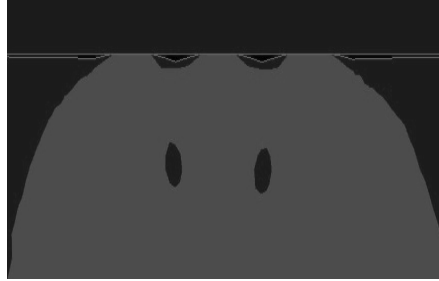


Figure 5. Plastic areas ($\sigma_{vm} < 300\text{Mpa}$)

3.1. Observation of the distribution of the von Mises stresses

While observing, during crushing, the areas evolving in a plastic way (von Mises stresses higher than the elastic limit of the material) Figure5, we can observe two singularities. The first one relates to the presence of areas that remain elastic even after the total crushing of the asperities. Indeed, these areas show hydrostatic compression aspects. The second relates to the appearance of a similar phenomenon localised between the asperities. The areas that remain in an elastic evolution during crushing are particularly interesting to study in order to understand the phenomena that appear during the static sealing. Indeed, they could attest presence of ways of leak during the flattening of two surfaces.

3.2. Observation of the strength depth curve

In order to study a modelling that allows the observation of the influence of the attack angle on the results, we propose geometry different from the preceding one. It is a four asperities problem whose attack angles are increasing by step of 1° . Thus, we will study three models. The first is relating to attack angles of 1° to 4° (rectified surface), the second one of 5° to 8° (milled surface), and finally, the third one of 9° to 12° (sanded surface). This study will thus enable us to observe the interactions between the asperities presenting different geometrical characteristics. Although the orders of magnitude relating to the curves presented in Figure 6 are closed to these induces by the crushing of a real surface, the shapes are different. As waited, the more the attack angle becomes acute, the more the plastic strain rate becomes significant.

We can also observe that the total strain energy decrease with the increase of the attack angles. These systems present an evolution much nearer to the framework of the experimental crushing, because the rates of elastic strain are more significant than the rates of plastic strain. Thus, the influence of the behaviour of the adjacent asperities significantly modifies the behaviour relating to a single asperity.

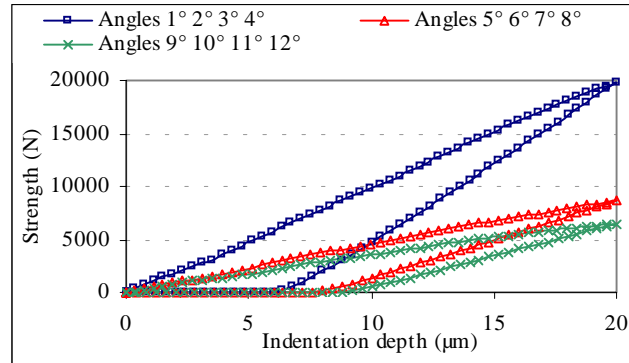


Figure 6. Strength/depth curve concerning the crushing of asperities presenting different rake angles

The study of the crushing of the asperities presents many difficulties, in particular with regard to the comprehension of the interactions phenomena between the entities. These phenomena depend on various parameters related to the topography of the system, but also to the behaviour of the material. We can note significant differences of the results according to the hardening mode adopted. For these reasons other studies showing the variations on the mechanical parameters must imperatively be carried out before being able to conclude on such phenomena.

Studying and understanding the phenomena governing the behaviour of a multi asperity system is a significant work, but to model the crushing of a surface in its entirety is as much. The finite elements cannot currently satisfy this need. To mesh and compute a simulation on a complete surface would require very significant resources in data-processing calculation. However, modelling such a simulation is possible by using simplifications made from numerical simulation, and by introducing the concept of representative strain.

3.3. Representative strain

Many works currently refer to the representative strain within the framework of the indentation of a plane by an indenter. The most famous result for a conical indentation is the relation $\varepsilon_r = 0.2 \cdot \tan(\beta)$ (Johnson, 1984). We propose now to define such an expression in the case of the crushing of an asperity. This strain will be given to be dependent on the minimum of parameters in order to be able to be applied to the greatest number of cases. This whole study is based on dimensional assumptions (Hanche-Olsen, 1998) related to the Vashy Buckingham's PI-theorem. In literature many studies were developed to deal with the indentation test (Bucaille

et al., 2003; Cheng *et al.*, 2000; 1999; Dao *et al.*, 2001). What we propose here is to do a similar work for the crushing of an asperity.

The expression of the evolution of the strength F function of the indentation depth h used to be:

$$F = Cb^3 \quad [2]$$

We can define such an expression related to the case of the crushing of an asperity:

$$F = K b^3 \text{ with } K = \frac{H_n \pi a^2}{b^2} \quad [3]$$

Where a is the contact radius and H_n the normal hardness of the material.

As we want this expression to be dependant on the minimum of parameters, let assume that the evolution of the indentation force is the following:

$$F = F(b, E^*, n, \sigma_r) \quad [4]$$

Where E^* is the reduced Young's modulus, n the hardness coefficient of the material, whose behaviour law is equation [1], σ_r is the representative stress which will allow us to introduce the representative strain concept. We need to find another expression for the force, function of a dimensionless quantity Π and a combination of the principal variables of the system h and σ_r . As Π is a dimensionless function, it can be expressed as:

$$\Pi = \frac{F}{\sigma_r b^2} \quad [5]$$

The Π function must depend on dimensionless quantities. That is the reason why it could be written as:

$$\Pi = f\left[\frac{E^*}{\sigma_r}, n\right] \quad [6]$$

With equations [3], [5] and [6] we can find the following relation:

$$\frac{K}{\sigma_r} = \Pi\left(\frac{E^*}{\sigma_r}, n\right) \quad [7]$$

This may not depend on the hardness coefficient (Hanche-Olsen, 1998). This assumption will allow us to find the representative strain. For various values of the hardness coefficient, we can obtain by finite element modelling the curves presented in Figure 7. As $\frac{K}{\sigma_r}$ depend on those coefficients [7], obtaining mixed curves ensures us to be independent of n , and thus to determine the value of the representative strain for a defined attack angle.

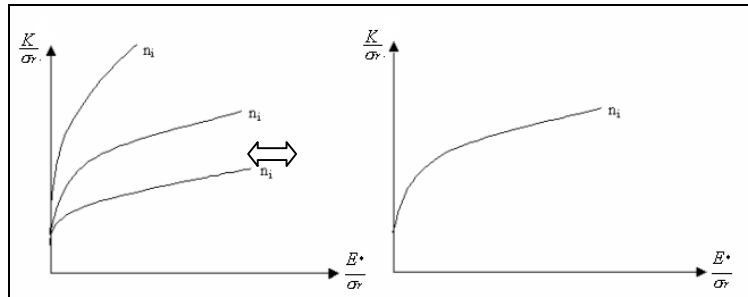


Figure 7. Mixed curves principle

These mixed curves are obtained by carrying out modifications on the value of σ_r and finding the maximum of correlation. Thus we can find ϵ_r using the following expression:

$$\sigma_r = \sigma_y \left[1 + \frac{E}{\sigma_y} \epsilon_r \right]^n \quad [8]$$

We performed 480 indentation tests with various material parameters (Young’s modulus, yield stress, hardening coefficient), and various geometries with modification of the rake angle. We verified that the results do not depend on the other geometrical parameters. Results are presented in Figure 8 and allow us to determine the expression of the representative strain for attack angles that varies from 1° to 10° .

$$\epsilon_r = 0.13 \tan(\beta) \quad [9]$$

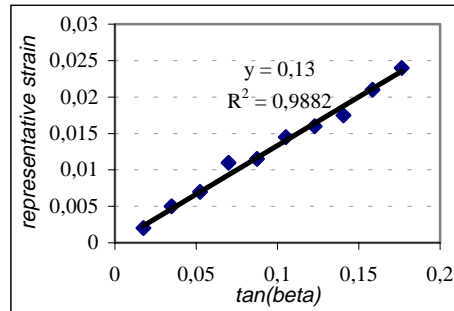


Figure 8. *Representative strain*

As finite elements cannot allow us to study a real flattening, we propose to use that representative strain concept in a new modelling way.

4. Conical model of the roughness

In this part of work, the roughness is considered as a distribution of conical indentors with various scale of attack angle (figure 9). For a conical tip geometry (Johnson, 1984), a nominal indentation strain is independent of the penetration depth of the indenter, it is only related to the attack angle β of the tip:

$$\varepsilon_m = 0.13 \tan(\beta) \quad [10]$$

In the case of an elastic contact, the mean pressure undergone by the asperity can be written:

$$p_m = 0.13E^* \tan(\beta) \quad [11]$$

The definition of the average deformation is introduced by taking into account of the average attack angle of the roughness $\bar{\beta}$.

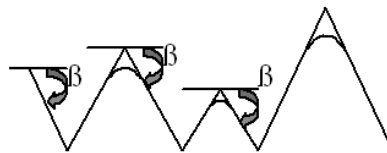


Figure 9. *Presentation of the roughness summits by cones*

The average pressure undergone by the asperities after quantification of the average attack angle of roughness, is written:

$$\varepsilon_m = 0.13E^* \tan(\bar{\beta}) \quad [12]$$

By analogy with the Greenwood model [10], we defined a new plasticity index (Jourani *et al.*, 2003) by considering the conical geometry of the roughness:

$$\Psi_{conc} = 0.13 \frac{E^*}{H} \tan \bar{\beta} \quad [13]$$

The deformations are elastic if $\Psi_{GW} < 0.6$ entirely plastic if $\Psi_{GW} > 1$ and elastoplastic for $0.6 < \Psi_{GW} < 1$.

4.1. Numerical model

The local behavior of each asperity is investigated numerically by means of the local summits geometry analysis. In this approach, we consider the contact between a perfectly smooth rigid plane and the local summits of the surface and neglect the elastic interaction between the asperities.

If the local area of the contact A_j between an asperity j and the plane is supposed elliptic, having semi-axes a_j and b_j given by (Ogilvy *et al.*, 1991), A_j is given by:

$$A_j = \pi a_j b_j \quad [14]$$

For a numerical solution, we discretize the local area A_j into N elements c_{ji} ($i = 1, 2, \dots, N$). In this case, the local pressure distribution on each asperity j , is given by the expression:

$$p_j(x_i, y_i) = \frac{3}{2} p_{jm} \left[1 - \left(\frac{x_i}{a_j} \right)^2 - \left(\frac{y_i}{b_j} \right)^2 \right]^{1/2} \quad [15]$$

Where p_{jm} the mean pressure undergone by the asperity j calculated by using the equation [2]

The normal force F_j exerted on an asperity j is given following relation:

$$F_j = \sum_i c_{ji} p_i \quad [16]$$

The total load supported by summits is:

$$F = \sum_j F_j \quad [17]$$

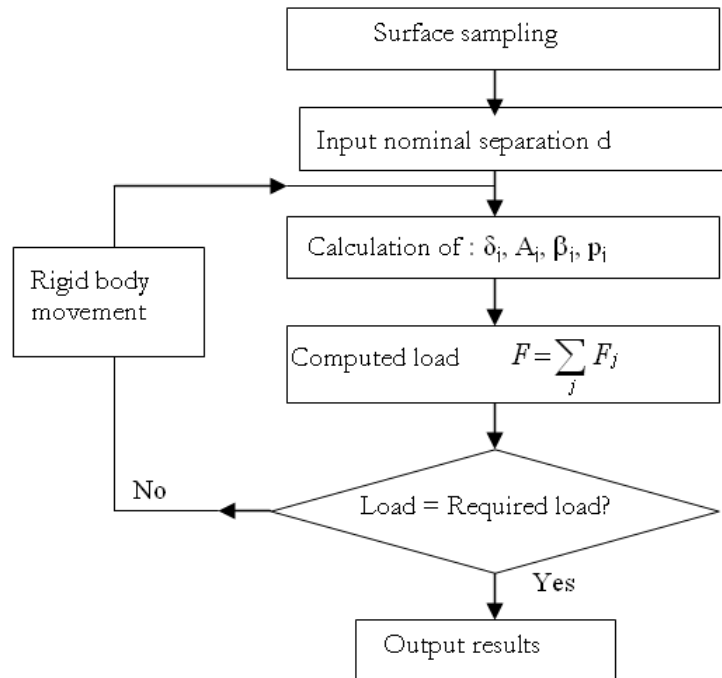


Figure 10. The algorithm used to calculate the parameters of contact

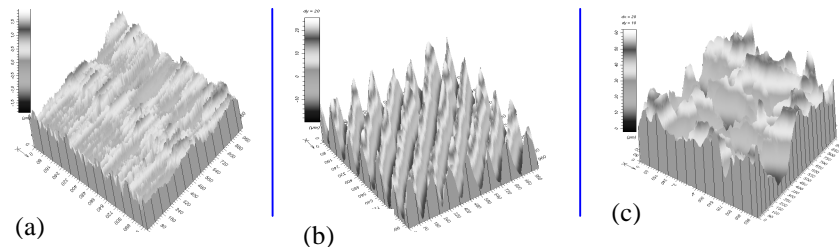


Figure 11. Topographies of real rough surfaces: (a) Ground surface, (b) milled surface; (c) sanded surface

Figure 10 is a flow chart for the contact calculation program. The three-dimensional surface topography is directly sampled by the computer-generated surface topography. For a given initial separation d , the local surface of the contact A_j , the local displacement d_j and the average attack angle β_j of each asperity can be determined. These parameters allow to determine the distribution of the pressure and the real contact area undergone by the roughness.

The analysis has been programmed in Matlab to study the contact between three rough surfaces of steel XC48 ($E = 210 \text{ GPa}; \nu = 0.3$) and a smooth rigid plane. The topographies of these surfaces are shown in Figure 11.

4.2. Numerical results

The calculated results are shown in Figure 12 and Figure 13. Figure 12 shows the pressure distributions for the three contact problems. In the case of the milled and sanded surface, pressure peaks reach 60-80 times the nominal contact pressure ($P_{\text{nom}} = 200 \text{ MPa}$), while in the case of ground surface the maximum pressure is only 8 times the nominal pressure. We can also observe that the mean contact pressures P_m (Table 1) increase with the increase of the attack angles. The comparison of these pressures with the hardness of the material ($H = 1280 \text{ MPa}$) allows to obtain an elastic behavior of *ground* surface and a plastic behavior of milled and sandblasted surface.

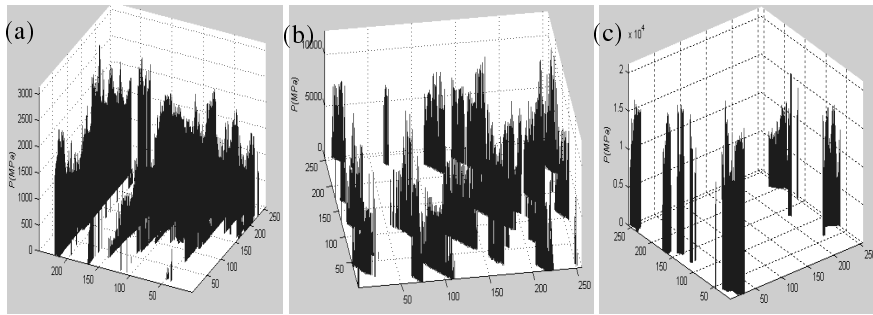


Figure 12. Pressure distributions. (a) Ground surface; (b) milled surface; (c) sandblasted surface

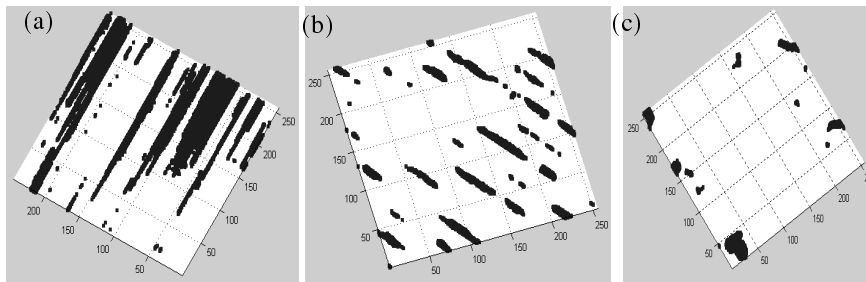


Figure 13. Distribution of real contact areas: (a) Ground surface; (b) milled surface; (c) sandblasted surface

The real contact area is much smaller than the nominal contact area (see Figure 13) and decreases with the increase of the attack angle. It is shown that for different contact surfaces, the distribution of real contact area is entirely different.

Table 1 presents the rate of the portance Ar , the mean contact pressure P_m , and plasticity index ψ_{cone} , calculated from the pressure distribution and the real contact area.

Table 1. Numerical results

Surface	Ra (μm)	β ($^\circ$)	P_m (MPa)	Ar (%)	ψ_{cone}
Ground	0.23	1.57	719	13.74	0.52
Milled	2.95	4.08	3830	5.35	1.37
Sanded	5.27	11.38	75683	2.23	3.87

To determine the parameters of contact, we can also use a model which considers the elastoplastic behaviour of the roughness. Following the pressure supported by the summit, we can distinguish three regimes of deformation (Figure 14):

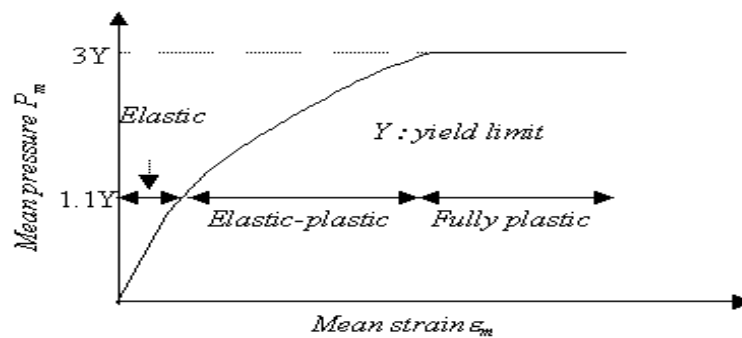


Figure 14. Different regimes of deformation (Johnson, 1984)

In the case of an elastic contact, the mean pressure undergone by the asperity can be written:

$$p_m = 0.2E' \tan(\beta) \quad [18]$$

If the contact is elastic-plastic, the mean pressure is given by:

$$p_m = \frac{2}{3} \left(1 + \tan \frac{E' \tan \beta}{3Y} \right) \quad [19]$$

When an asperity is deformed plastically, the mean pressure is given by the hardness of the substrate H:

$$p_m \approx 3\sigma_y \approx H \quad [20]$$

5. Experimental validation of the Numerical model

To discuss the validity of this model, a device of indentation of rough surfaces (Jourani *et al.*, 2003) was developed. This experimental device gives us the evolution of the contact forces during the load and unload process. Figure 15 shows the load and unload curves on the three surfaces used previously. The applied nominal contact pressure is $P_{nom} = 200\text{MPa}$.

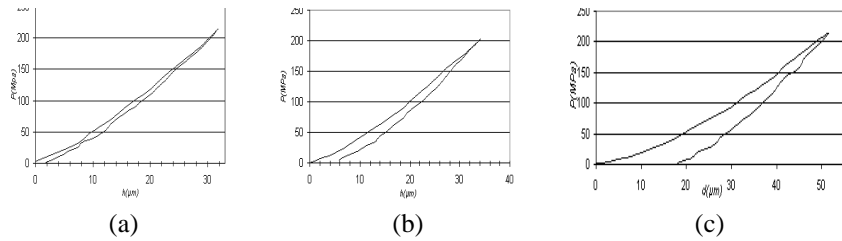


Figure 15. Indentation curves: (a) Ground surface, (b) milled surface; (c) sanded surface

The analysis of these experimental curves allows to determine the residual plastic displacement, plastic and elastic energy. The results are grouped in Table 2.

Table 2. Experimental results

Surface	Ground	Milled	Sanded
Residual plastic displacement (μm)	1.63	5.7	17.91
Rate of elastic energy (%)	7	15	31
Rate of plastic energy (%)	93	85	69

The attack angle of the roughness influences the elastic and plastic behaviour of the surfaces. Indeed, for the same nominal contact pressure, the elastic and plastic

energy are completely different. Ground surface has a quasi elastic behaviour with a residual plastic displacement equal to $1.63\mu\text{m}$. Milled and sanded surfaces present, on the other hand, a plastic behaviour more marked with residual plastic displacement respectively equal to $5.7\mu\text{m}$ and $17.91\mu\text{m}$.

These numerical results are in agreement with the model of conical roughness and validate the numerical model developed above.

6. Conclusions

In this work we carried out numerical simulations by finite elements modelling on a microscopic scale showing the importance of local slopes in contact between rough surfaces. These simulations make it possible to observe the evolution of the elastic-plastic behaviour of the surface according to various parameters such as the attack angle of the asperities, considered as conical, and behaviour law associated with the system.

Thus, to be able to deal with the three dimensional contact, we developed a new method based in the modelling the local roughness as a distribution of indentors with various attack angles, in contact with a smooth rigid plan. It enables us to obtain the local distributions of the pressures, the real contact area as well as the surface deformed during the flattening. The methodology can be extended to the spectral analysis of the slopes of roughness, in order to study the incidence of the scales of roughness and fractal properties in the creation of singular pressures.

Acknowledgements

The authors make a point of thanking CNRS and the industrialists of the GDR 2 345 (Etanchéité statique en Milieux Extrêmes) for the financial support and the profitable exchange during this project.

7. References

- Bucaille J.L., Strauss S., Felder E., Michler J., "Determination of plastic properties of metals by instrumented indentation using different sharp indenters", *Acta Mater.*, Vol. 51, Issue 6, 2003, pp. 1663-1678.
- Cheng YT, Cheng CM., "Scaling relationships in conical indentation of elastic-perfectly plastic solids", *International Journal of solids and Structure*, Vol. 36, 1999, pp. 1231-1243.
- Cheng YT, Cheng CM, "What is indentation hardness?", *Surface and coatings Technology*, Vol. 133-134, 2000, pp. 417-424.

Dao, Chollacoop N., Van Vliet K.J., Venkatesh T.A., Suresh S., “Computational modelling of the forward and reverse problems in instrumented sharp indentation”, *Acta mater*, Vol. 49, 2001, pp. 3899-3918.

Greenwood J.A., Williamson J.B.P., “Contact of nominally flat surfaces”, *Proceedings of the Royal Society* 295, 1966.

Hanche-Olsen H., “Buckingham’s pi-theorem”, *Internet document*, 1998.

Johnson K.L., *Contact mechanics*, Cambridge University Press, Chap. 6, *Normal Contact of Inelastic solids*, 1984.

Jourani A., Hamdi H., Dursapt M., Delalleau A., Zahouani H., “Elastoplastic behaviour of roughness during a static contact between solids”, *16th Mechanical French congress 2003*, Nice, France.

Ogilvy J.A., “Numerical simulation of friction between contacting rough surfaces”, *J.Phys. D:Appl. Phys.*, 24, pp. 2098-2109, 1991.

SYSTUS® version 2004, User manual, ESI group.